Applicability and quality of linear stability theory and linear PSE in swept laminar separation bubbles

Tilman Hetsch and Ulrich Rist

Institut für Aerodynamik und Gasdynamik, Universität Stuttgart,
Pfaffenwaldring 21, 70550 Stuttgart, Germany.
`hetsch@iag.uni-stuttgart.de`

Summary

A family of laminar separation bubbles (LSB) in a swept boundary layer flow - hereafter referred to as "swept LSB"- is used to study the effect of sweep and of the propagation direction of disturbance waves on the quality of linear stability theory (LST) and solutions of the parabolized stability equations (PSE). To this end spatial LST and linear PSE solutions are qualitatively and quantitatively compared to highly resolved results of direct numerical simulations (DNS). The sweep angle of the base flow is systematically varied between $0°$ and $45°$ and a variety of Tollmien-Schlichting waves as well as the most amplified stationary cross-flow mode are investigated. It turns out, that even though LST works satisfactory in the presence of sweep, flow separation and back flow, PSE is clearly preferable in terms of accuracy.

1   Introduction

Since the nineties linear PSE-methods are increasingly used for similar tasks as the traditional spatial LST. In aircraft industry their most important field of application lies in the semi-empirical e^N-method for transition prediction, where nowadays both methods are utilised, as for example in [5]. In research, either method provides an inexpensive a priori analysis of single modes or the whole flow field in form of stability diagrams, if base flow is steady. Thus purposeful disturbance scenarios can be determined in advance of computationally more demanding methods like DNS ([6], p. 60). For unsteady flows at least a posteriori analysis of the time averaged DNS-flow field is possible, as done in [3], p. 140. Finally, both methods are frequently used for the validation of codes and measurements.

All these applications depend on the ability of LST and PSE to model the propagation of low amplitude disturbances realistically. Laminar separation bubbles (LSB) represent a demanding base flow for both methods. One might expect problems with non-parallel effects due to curved streamlines and the rapid growth of the boundary layer thickness over the bubble in the case of LST and with the back flow inside the bubble for the streamwise marching procedure on which the efficiency of PSE rests on. But for *unswept* LSB this poses no problem: Over the last decade LST has been very successfully applied to LSB in 2D-base flows (see e.g. [4], [3]

and references therein). For PSE growth rates good agreement was also achieved by Hein in [1] (see figure 1 in [1]) compared to DNS results of the unswept version of the same leading edge bubble investigated here. Still unknown on the other hand is the general applicability and overall quality of LST and PSE in laminar separation bubbles in a swept, three-dimensional flow. This is investigated in detail for Tollmien-Schlichting modes in section 3 with emphasis on the effect of sweep and for the linearly most amplified cross-flow mode in section 4. Throughout the paper PSE always refers to linear PSE and LST/DNS to spatial LST/DNS.

2   Base flow and numerical methods

The unswept prototype of the present leading edge bubble was extensively studied by Rist in [4] by means of DNS and LST. Its extension to swept flows, the verification of the base flow by step size tests, as well as the effect of sweep on the base-flow profiles and a first LST analysis were reported by Hetsch & Rist in [2]. The DNS calculations are split in a DNS of the steady laminar base flow and a succeeding DNS for the disturbance propagation. These two DNS-codes solve the complete three-dimensional Navier-Stokes equations for unsteady, incompressible flows in a vorticity-velocity formulation. For an in-depth description of the DNS algorithms see [6]. The LST-code used here is the same as in all three references above. The PSE-results were obtained by the code "nolot" of the DLR-Göttingen, described in [1]. All PSE-calculations were started with local solutions obtained from LST.

The most important base flow parameters described in [2] are repeated here: All quantities in the paper are non-dimensionalized by the reference length $\overline{L} = 0.05\,\mathrm{m}$ and the chordwise free-stream velocity $\overline{U}_\infty = 30\,\frac{\mathrm{m}}{\mathrm{s}}$, which is held constant for all cases. The x- and z-direction are taken normal and parallel to the leading edge with U and W being the associated base flow velocity components, respectively. Periodicity is assumed in spanwise direction only, resulting in a quasi-2D base flow with $(\frac{\partial}{\partial z} \equiv 0)$, but $W(x,y) \neq 0$. The calculation domain itself consists of an infinite flat plate subjected to an adverse pressure gradient. It is introduced to the system by prescribing the chordwise potential flow velocity $U_e(x)$ shown in Figure 1 at the upper boundary of the domain. Different sweep angles Ψ are realized by varying the spanwise free stream velocity $W_\infty = U_\infty \tan(\Psi)$ and setting $W_e(x) \equiv W_\infty$. At the inflow located at $x_o = 0.37$ Falkner-Scan-Cooke profiles are prescribed. With a kinematic viscosity of $\overline{\nu} = 15 \cdot 10^{-6}\frac{\mathrm{m}^2}{\mathrm{s}}$ the flow can be characterised by $Re_{\delta_1} = \overline{U}_\infty \overline{\delta}_1(x_o)/\overline{\nu} = 331$, based on the displacement thickness. The wall-normal coordinate y ranges from 0 to $y = 0.059 = 18 \cdot \delta_1(x_o)$ with $y = \overline{y}/\overline{L}$.

Thus, a family of swept LSB with arbitrary sweep angle is obtained, which –in agreement with the independence principle of infinite swept geometries, see [2]– have identical separation and reattachment positions at $x_s = 1.75$ and $x_r = 2.13$, respectively. The steady calculation of the separation bubble is justified by its small size (e.g. the maximum back flow is $0.3\,\%\,\overline{U}_\infty$) and experience with the unswept case in [4]. It is converged to steady state, if the differences in V and the vorticity components Ω_x and Ω_z of two consecutive time levels are smaller than 10^{-10}.

3 Tollmien-Schlichting waves

For the investigation a packet of Tollmien-Schlichting (TS) waves with varying spanwise wavenumber $\gamma \in [-40, -30, -20, 0, 20, 30, 40]$ was excited by a disturbance strip displayed in Figure 1. They all share the most amplified frequency $\omega = 18$ of the $0°$-base flow. In the following the notation (ω/γ) is adopted for discrete modes in the frequency-spanwise wavenumber spectrum. Small initial amplitudes of $A_v = 10^{-10}$ grant a purely linear development throughout the domain. Figure 2 shows two examples of amplification curves $u'_{\omega,\gamma}(x) = \max_y(\widehat{A}^u_{\omega,\gamma}(x,y))$, where $\widehat{A}^u_{\omega,\gamma}$ denotes the amplitude of a double Fourier analysis of the disturbance velocity component u' in time and span. Local DNS-amplification rates may be obtained by $\alpha_i[DNS] := -d(\ln u'_{\omega,\gamma})/dx$. For quantitative comparison local amplification rates α_i obtained by LST are integrated to calculate the amplification curve $A_o\, e^{-\int \alpha_i\, dx}$. Its initial amplitude A_o is fitted to match the DNS results around the neutral point $x_{neut} = 0.95$ (see Fig. 2), after which most modes are amplified for the first time. The relative error $r_{rel} := |DNS - LST|/DNS$ was then evaluated at $x_{DNS-max}$, the position of the peak of the DNS-amplification curve shown in Figure 2. Here the greatest N-factor, defined as $N(x) := \int_{x_{neut}}^{x} -\alpha_i\, dx$, is achieved. All findings were compiled into table 1. Analogous results for PSE are found as a second entry in same table. Table 2 gives the propagation angle $\Psi = \arctan(\gamma/\alpha_r)$ of all modes in a body-fitted and a streamline orientated coordinate system, α_r representing the chordwise wavenumber. For most modes Ψ changes only little in the present base flow, so those values can be regarded as typical.

The effect of sweep: The relative error of the LST-amplification curves is quite high. On the average it was found to be 40% for the $0°$-base flow and about 50% for the sweep angles $\Psi_\infty = 30°$ and $45°$. All in all there is a tendency towards higher errors for increasing sweep angles Ψ_∞. Note that $45°$-mode $(18/-40)$ displays a slightly atypical behaviour in table 1, as it is nearly neutrally stable. LST was applicable for the whole range of $\Psi_\infty \in [0°, 45°]$, but the modes $(18/\pm 40)$ showed first, still negligible convergence problems in their damped regions for $\Psi_\infty = 45°$. The attempt to calculate a complete stability diagram by LST in a $60°$ bubble failed due to heavy convergence problems already in the amplified regions of the flow. PSE on the other hand was able to predict the disturbance development starting at the neutral point with a relative error of only 6% in the mean, nearly unaffected by Ψ_∞. In the $45°$-case beginning convergence problems made it necessary to double the step size for the modes $(18/30)$ and $(18/40)$. This coarse discretisation led to higher errors compared to other PSE-results.

The effect of the propagation direction: Table 2 reveals that the propagation direction Ψ grows monotonically with the spanwise wavenumber γ. The general trend for LST "larger errors for more oblique modes with larger $|\gamma|$ and therefore larger $|\Psi|$" is much more pronounced than the effect of a rising sweep angle. The smallest relative errors of $16\% - 19\%$ are found for modes around $\gamma = 0$. For very oblique

modes within the same base flow the errors are up to 4 times higher. Note that there is *no* trend "larger errors for modes with larger $|\gamma_s|$" with respect to the angle Ψ_s relative to the direction of the potential stream line. Obviously, in the 45°-case the TS-wave $(18/30)$ with the smallest angle in the stream-line orientated coordinate system does not exhibit the minimal error. PSE shows also the tendency for higher errors for more oblique modes, but much less pronounced than for LST.

LST for local quantities and qualitative comparison: The high relative errors listed in table 1 should not discourage the use of LST in swept LSBs. Fitting the curves at the neutral point is necessary in the context of N-factor calculation, but shows the *integrated* error from there up to the point of comparison. The direct results of LST are *local* ones –growth rates, wavelengths, propagation directions– for which only the error at the place of comparison is taken into account. Also, many applications of LST mainly require *qualitative* comparisons of curves. This yields improved results, because the curves are fitted at an arbitrary point, for which the error is equally distributed over the whole length of the domain. Furthermore comparison with linear theories are only meaningful until one mode reaches the critical amplitude value of about $1\% U_e$ where nonlinear effects should not be neglected any longer. Therefore, the interval of comparison will typically be smaller than analysed here. An example of a nonlinear scenario is shown in Figure 3, where the LST of the dominating mode $(18/0)$ shows excellent agreement up to the point of saturation and even the mode $(18/40)$ with the extremely high relative error of 78% (at its peak at $x \approx 2.25$) compares more or less satisfactory within the linear regime.

4 Stationary cross-flow modes

In the 45° base flow the strength of the crossflow (CF) velocity W_s, the spanwise base flow velocity in a streamline orientated coordinate system, reaches a value of about $W_{s,max}/U_{s,max} = 8\%$ relative to its streamwise counterpart U_s. Furthermore, W_s-profiles exhibit an inflection point indicating the influence of an inviscid crossflow instability. LST was used to determine the most amplified stationary CF-mode. The maximal growth rates α_i of stationary CF-modes inside the LSB were found to be roughly one-third of those of the most amplified TS-waves. The strongest amplification was exhibited by the modes $(0/40)$ and $(0/50)$, which showed nearly identical amplification curves. The $(0/40)$ was chosen for further comparison. As displayed in Figure 4, the LST- and PSE-amplification curves were individually fitted to the DNS-result in order to achieve the best overall match. After a short transient phase PSE yields excellent agreement with the DNS solution, whereas LST looks even qualitatively less convincing than for the TS-waves from section 3. On the other hand the y-scale is much larger here. Other authors also indicate that LST fails to give good quantitative results in the case of CF-modes. Wassermann and Kloker for example examined several CF-modes in an accelerated 45°-boundary layer without separation in [6]. They report that the LST systematically underpredicts the DNS-growth rates, a trend which is also observable in Figure

2 for the TS-waves investigated here. In their study amplification curves of DNS and LST differed at the middle of the domain already by a factor of $3 - 4$.

5   Conclusion

The applicability and accuracy of linear stability theory and linear PSE was investigated for a generic family of small laminar separation bubbles. LST and PSE were found to be applicable in the whole sweep angle range of $\Psi_\infty \in [0°; 45°]$. As both methods showed beginning convergence problems in the $45°$-base flow increasing difficulties can be expected for higher sweep angles. A packet of TS-waves with systematically varying spanwise wave number γ was compared to DNS-results for all sweep angles. In terms of accuracy PSE is clearly superior to LST, which systematically underpredicts the DNS-growth rates. Compared to DNS-amplification curves the mean error over all modes and sweep angles yielded 6% for PSE compared to 46% for LST. An error of 64% already results in an amplitude factor difference of 2.8 between LST and DNS, which would correspond to a $\Delta N = 1$ in a N-factor prediction. On the other hand the amplification in LSBs is so extreme compared to attached boundary-layer flows –the maximum growth rate of the present LSB is 16 times higher than that of the same inflow without pressure gradient– that even such an error might result in only a small Δx-shift of the predicted transition location.

LST was found to work best for $0°$-base flows. The errors increased with rising sweep angle, in the mean by a factor of 1.25 from $\Psi_\infty = 0°$ to $45°$. More pronounced is the dependency of LST from the propagation direction Ψ of the analysed mode. It exhibited the general trend "larger errors for modes with larger propagation angles". In the present investigation the errors of the most oblique waves were up to 4 times higher than errors for two-dimensional waves. The accuracy of *PSE*-results on the other hand was rather independent of the sweep angle. But oblique waves with the largest propagation angle also showed the maximum errors. In the mean they differed from the minimum error of the mode $(18/-20)$ by a factor of 1.75.

In application LST is very robust and easy to handle and automate because of its local character. It is well suited to get an overview, for the qualitative comparison of curves or when a great number of modes has to be calculated, as for stability diagrams. Due to its step-size restriction PSE requires more attention per run. PSE comes into play when greater accuracy is desired and is clearly superior for CF-modes. Note that the present base flow was a flat-plate boundary layer. In curved geometries, PSE has the additional advantage of the inclusion of curvature terms.

Acknowledgements

References

[1] S. Hein: "Linear and nonlinear nonlocal instability analyses for two-dimensional laminar separation bubbles". Proc. IUTAM Symp. on Laminar-Turbulent Transition, Sedona, USA, Sep. 1999, Springer, p.681-686.

[2] T. Hetsch, U. Rist: "On the Structure and Stability of Three-Dimensional Laminar Separation Bubbles on a Swept Plate". In: Breitsamter, Laschka et al. (ed.): 13th STAB Symposium 02, Munich. NNFM **87**, Springer 2004, pp. 302-310.

[3] O. Marxen, M. Lang, U. Rist, S. Wagner: "A Combined Experimental/Numerical Study of Unsteady Phenomena in a Laminar Separation Bubble". Flow, Tub. and Comb. **71**, Kluwer Acad. Pub., 2003, pp.133-146.

[4] U. Rist: "Zur Instabilität und Transition in laminaren Ablöseblasen". Habilitation, Universität Stuttgart, Shaker 1999.

[5] G. Schrauf: "Industrial View on Transition Prediction". In: S. Wagner et al. (ed.): "Recent Results in Laminar-Turbulent Transition". NNFM **86**, Springer 2003, pp. 111-122.

[6] P. Wassermann, M. Kloker: "Mechanisms and passive control of crossflow-vortex-induced transition in a three-dimensional boundary layer". J. Fluid Mech. **456**, Camb. Univ. Press 2002, pp.49-84.

Table 1   First number: Relative error $\mathrm{r}_{\mathrm{rel}} := |DNS - LST|/DNS$ of LST results in per cent with respect to DNS amplification curves, evaluated at X-position of greatest amplification of the DNS-curve (see Fig. 2). Its dependency on various modes (ω/γ) (columns) and sweep angles Ψ_∞ of the base flow (rows). Second number: Same findings for PSE.

Ψ_∞	(18/-40)	(18/-30)	(18/-20)	(18/0)	(18/20)	(18/30)	(18/40)	mean
0°	58 / 8	55 / 6	16 / 5	16 / 4	16 / 5	55 / 6	58 / 8	39 / 6
30°	51 / 6	58 / 4	58 / 6	19 / 5	15 / 1	62 / 6	73 / 2	48 / 4
45°	25 / 6	51 / 2	59 / 2	19 / 5	39 / 9	81 / 10	78 / 11	50 / 6
mean	45 / 7	55 / 4	44 / 4	18 / 5	23 / 5	66 / 7	70 / 7	46 / 6

Table 2   Propagation angle $\Psi = \arctan(\gamma_r/\alpha_r)$ in degrees with respect to the X-axis of modes in table 1 according to LST at $x = 1.4$. Second number: Propagation angle $\Psi_s = \arctan(\gamma_r/\alpha_{r_s})$ in streamline orientated coordinate system, displayed in Figure 1.

| Ψ_∞	(18/-40)	(18/-30)	(18/-20)	(18/0)	(18/20)	(18/30)	(18/40)
0°	-41	-32	-22	0	22	32	41
30°	$-30/-61$	$-25/-56$	$-19/-49$	$0/-31$	$27/-4$	$43/12$	$58/28$
45°	$-25/-71$	$-22/-67$	$-17/-62$	$0/-46$	$32/-14$	$54/8$	$79/33$
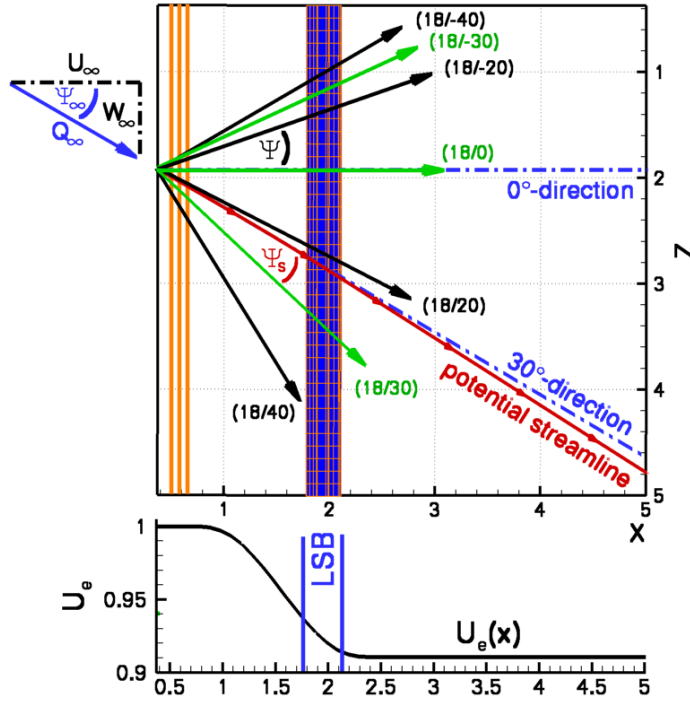
Figure 1 $30°$-base flow: Topview. Disturbance strip $x \in [0.5; 0.64]$, LSB between $x_s = 1.75$ & $x_r = 2.13$, potential streamline. Propagation direction Ψ of investigated TS-waves (ω/γ) according to LST at $x = 1.4$. Smaller Figure: potential chordwise velocity $U_e(x)$.
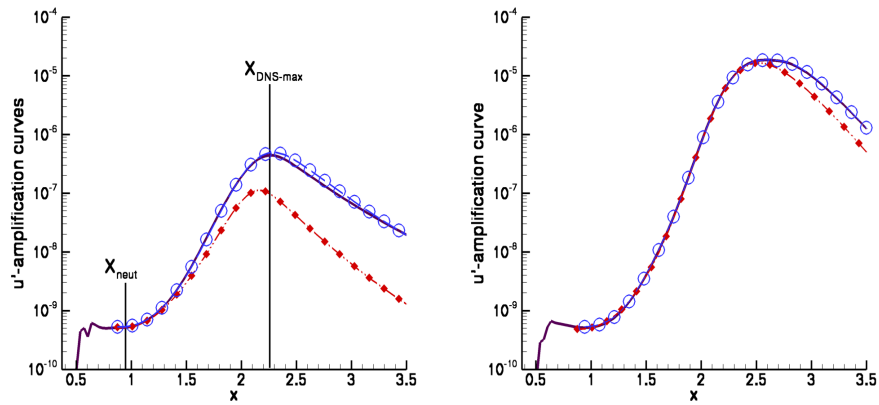
Figure 2 Amplification curves. Left: $(18/40)$ in $45°$-base flow with x-positions of error evaluation in section 3 (example of high relative error compared to other TS-waves). Right: $(18/20)$ in $30°$-base flow (lowest relative error). Lines: DNS, diamonds: LST, circles: PSE.
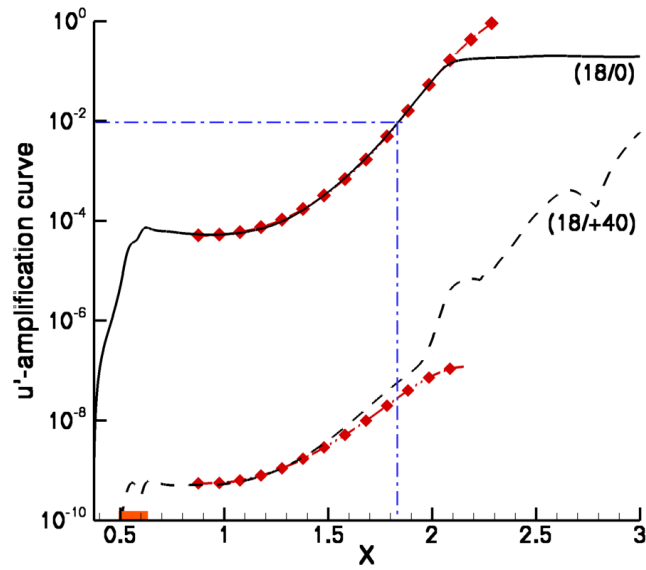
Figure 3 $45°$-LSB nonlinear scenario: Dominating disturbance $(18/0)$ with initial amplitude $A_v = 10^{-5}$, all other modes: $A_v = 10^{-10}$, shown only $(18/40)$. End of linear regime at $x \approx 1.8$ indicated by dash-dotted lines. Lines: DNS, diamonds: LST.
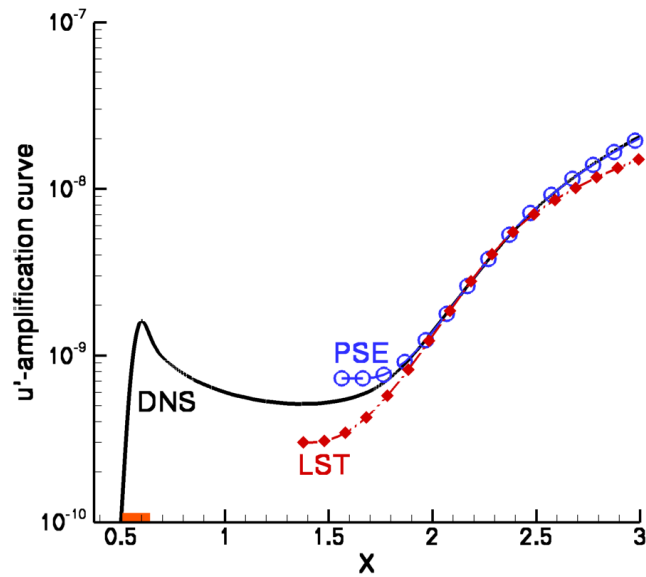
Figure 4 $45°$-LSB: Linearly most amplified stationary CF-mode $(0/40)$ with disturbance strip. Initial amplitude: $A_v = 10^{-10}$. Lines: DNS, diamonds: LST, circles: PSE.